$e[E_{1/2}(ox) - E_{1/2}(red)]$, $E_{1/2}(ox)$ and $E_{1/2}(red)$ are the oxidation and reduction potentials of the complex, and A and B are terms that correct for the solvation energies, inner- and outer-sphere barriers, and Coulombic energies. The relationship between the absorption/emission maxima and the electrochemical potentials shows that the redox and spectroscopic orbitals are the same.

Protonation of the pyrazine ring causes a decrease in energy of the $d\pi-\pi^*$ transitions. Resonance Raman measurements have revealed that the low-energy band at 530 nm belongs to a $d\pi \rightarrow \pi^*$(pyrazinyltriazole) transition, while the band at 400 nm is due to a $d\pi \rightarrow \pi^*$(bpy) transition. Protonation of the free nitrogen in the pyrazine ring causes a stabilization of the π^* orbital.[7] This will cause a more efficient π back-bonding from the ruthenium ion to the ligand. The electrochemical measurements indicate that after protonation of the pyrazine ring the ligand becomes a stronger π-acceptor[2] and a weaker σ-donor ligand. Less electron density is present on the ruthenium ion, and it is more difficult to oxidize the protonated complex.

There are two possible explanations why no emission is observed for the complexes in sulfuric acid: the emission maxima were present at lower energy than could be measured with our equipment (800 nm was the low-energy limit) or the complexes with a protonated pyrazine ring do not emit at all. This is unlike ruthenium compounds with bipyrazine and tetraazaphenanthrene, which are still emitting compounds after protonation.[7,9] The weaker σ-donor capacities of the protonated pyrazinyltriazole ligand cause a decrease in the ligand field strength, and a lower ^{3}MC state is expected. Therefore, a decrease in the quantum yield of the emission is observed.[3]

Conclusions. The electrochemical and spectroscopic data obtained for the ruthenium compounds containing the pyrazinyltriazole ligands HL0, L1, L2, and HL3 clearly indicate that in the complexes the LUMO's of the pyrazinyltriazole ligands are lower than the LUMO of bpy. Upon deprotonation of the complexes with HL0 and HL3, the LUMO of the compounds are now located on the bpy ligands. The emission data (energies and lifetimes) indicate that in $[Ru(bpy)_2(L)]^{2+}$ (L = HL0, L1, L2, and HL3) the pyrazinyltriazole ligands are most likely involved in the emission process, whereas the emission of $[Ru(bpy)_2(L0^-)]^+$ and $[Ru(bpy)_2(L3^-)]^+$ is bpy based.

Up till now, two types of acid-base behavior have been described for ruthenium(II) compounds. Class a compounds show a red shift of the absorption and emission maxima upon protonation of the coordinating ligands. Examples are ruthenium complexes with 2,2'-bipyrazine,[7] 2,3-bis(2-pyridyl)pyrazine,[38] [4,7]-phenanthrolino[5,6-*b*]pyrazine,[38] and 1,4,5,8-tetraazaphenthrene.[9] This red shift upon protonation of the ligands has been explained by stabilization of the π^* orbital.

The absorption and emission spectra of class b compounds are blue-shifted when protonated. Examples are $Ru(bpy)_2$ complexes with imidazole[38,39] pyrazole,[16] and 1,2,4-triazole[5,10] anions. Upon protonation of the ligands, less electron density is present at the metal center and therefore the filled $d\pi$ orbital is stabilized. This results in a larger energy difference between the $d\pi$ and the π^* orbitals.

A combination of above-mentioned effects is observed for the ruthenium complexes with the $L0^-$ and $L3^-$ ligands; when protonated, the filled $d\pi$ orbitals, as well as the π^* level of the pyrazinyltriazole ligand, are lowered. After protonation, the pyrazinyltriazole π^* orbital becomes just lower than the π^* orbital of bpy. Therefore, a combination of a higher oxidation potential and a less negative reduction potential is observed. This causes a rather small energy difference between the protonated and deprotonated species, which is reflected in the energies of the absorption and emission spectra of the protonated and deprotonated complexes.

Acknowledgment. We thank Johnson Matthey Chemical Ltd. (Reading, U.K.) for their generous loan of $RuCl_3$. We wish to thank Unilever Research Laboratories (Vlaardingen, The Netherlands) for the use of the electrochemical equipment. Part of the emission measurements were performed in Bologna, Italy, during a stay of R.H. Dr. F. Barigelletti, Prof. V. Balzani, and Dr. L. De Cola are thanked for useful discussions.

(38) Hosek, W.; Tysoe, S. A.; Gafney, H. D.; Baker, A. D.; Strekas, T. C. *Inorg. Chem.* **1989**, *28*, 1228.
(39) Haga, M. *Inorg. Chim. Acta* **1983**, *75*, 29.

Contribution from the Departamento de Quimica Fisica, Facultad de Quimica, Universidad de Barcelona, 08028-Barcelona, Spain, Department of Chemistry, North Carolina State University, Raleigh, North Carolina 27695-8204, and Chemistry and Materials Science Divisions, Argonne National Laboratory, Argonne, Illinois 60439

Interaction Energies Associated with Short Intermolecular Contacts of C-H Bonds. 1. Ab Initio Computational Study of C-H···Anion Interactions, C-H···X^- (X^- = I_3^-, IBr_2^-, ICl_2^-)

Juan J. Novoa,*[,†,‡] Fernando Mota,[†] Myung-Hwan Whangbo,*[,§] and Jack M. Williams*[,∥]

Received March 15, 1990

The nature of the C-H···anion contact interactions found for organic charge-transfer salts was investigated by performing SCF-MO and MP2 level calculations on the model systems $H_3C-H\cdots Y-I-Y^-$ (Y = I, Br, Cl). The binding energies of the $H_3C-H\cdots Y-I-Y^-$ systems are estimated to be 1.1, 1.3, ad 1.6 kcal/mol for Y = I, Br, and Cl, respectively. The binding energy increase, observed when Y varies from I to Br to Cl, is consistent with the expected hydrogen-bonding abilities of the halogen atoms. The C-H bond prefers to make a short contact with the terminal halogen atoms of Y-I-Y^-; this tendency increases as Y changes from I to Br to Cl, and the $C-H\cdots Y-I-Y^-$ interaction energies do not strongly depend upon the C-H···Y contact angle.

Organic donor molecules bis(ethylenedithio)tetrathiafulvalene (BEDT-TTF, **1**) and its analogues form 2:1 charge-transfer salts with a variety of monovalent anions X^-.[1] Several BEDT-TTF salts are ambient-pressure superconductors, which include β-$(BEDT-TTF)_2X$ (X^- = I_3^-, AuI_2^-, and IBr_2^-, for which the superconducting transition temperature T_c = 1.4,[2] 5.0,[3] and 2.8 K,[4] respectively) and κ-$(BEDT-TTF)_2X$ (X^- = $Cu(NCS)_2^-$ and I_3^-,

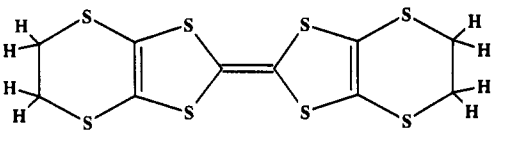

1

† Universidad de Barcelona.
‡ On leave of absence at North Carolina State University.
§ North Carolina State University.
∥ Argonne National Laboratory.

0020-1669/91/1330-0054$02.50/0

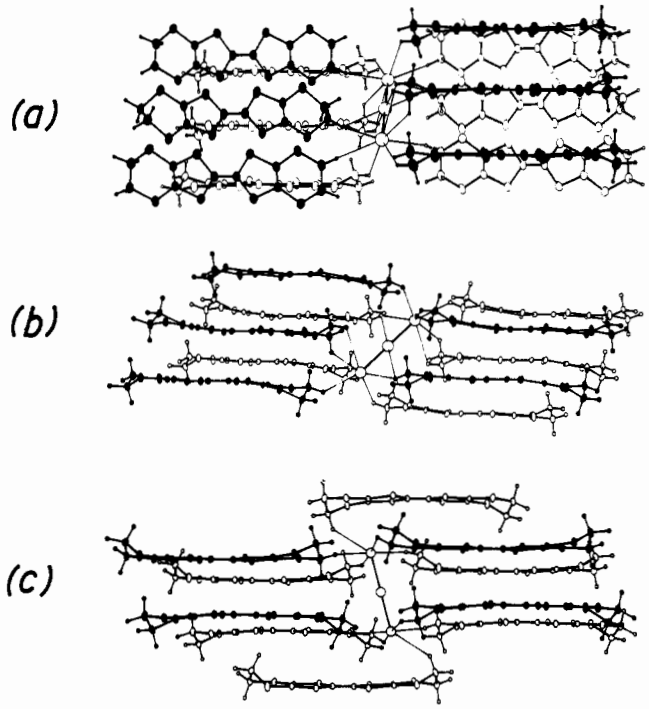

Figure 1. Perspective views of the hydrogen pockets surrounding the Y–I–Y⁻ anions in (a) α-(BEDT-TTF)$_2$I$_3$, (b) β-(BEDT-TTF)$_2$IBr$_2$, and (c) β-(BEDT-TTF)$_2$ICl$_2$.

for which T_c = 10.4[5] and 3.5 K,[6] respectively). Most 2:1 charge-transfer salts of BEDT-TTF have a layered structure in which layers of donor molecules alternate with layers of anions and the π-framework of each donor molecule is inclined with respect to the anion layers. Thus, the C–H bonds at both ends of BEDT-TTF make short contacts with the anions such that each anion is surrounded in a hydrogen pocket made up of the donor-molecule ethylene groups.[1] This is illustrated in Figure 1 for the linear triatomic anions X⁻ = I–I–I⁻, Br–I–Br⁻, and Cl–I–Cl⁻ found in α-(BEDT-TTF)$_2$I$_3$,[7] β-(BEDT-TTF)$_2$IBr$_2$,[4] and β-(BEDT-TTF)$_2$ICl$_2$.[8] In the hydrogen pockets there also occur short C–H···H–C contacts, though not shown for simplicity.[9]

Whether the charge-transfer salts are semiconducting, metallic, or superconducting depends upon the electronic and vibronic properties associated with the packing patterns of their molecule layers. The latter in turn are governed by the donor···donor and donor···anion interactions involving the C–H bonds of the donor molecules.[9,10] For instance, these C–H···donor and C–H···anion interactions provide a key to understanding the anion and pressure dependence of the T_c values of β-(BEDT-TTF)$_2$X (X⁻ = I_3^-, AuI_2^-, IBr_2^-),[9,11] the thermal conversion of α-(BEDT-TTF)$_2$I$_3$ to α_t-(BEDT-TTF)$_2$I$_3$,[12] and that of δ-(BEDT-TTF)$_2$AuBr$_2$ to α'-(BEDT-TTF)$_2$AuBr$_2$.[13] As part of our ongoing research on the C–H···donor and C–H···anion interactions, the present work examines the nature of the C–H···anion interactions associated with the anions I–I–I⁻, Br–I–Br⁻, and Cl–I–Cl⁻ by performing ab initio SCF–MO and nth order Moller–Plesset[14] (i.e., MPn, n = 2–4) correlation energy calculations on the model systems H_3C–H···Y–I–Y⁻ (Y = I, Br, Cl) (see **2** and **3** for the geometrical arrangements of CH_4 and Y–I–Y⁻).

Table I. Exponents for the Polarization and Diffuse Functions Used in PSHONDO and GAUSSIAN 86 Calculations

	polarization	diffuse		polarization	diffuse
C	0.75	0.0340	Br	0.371	0.0500
H	1.0	0.0360	Cl	0.580	0.0490
I	0.250	0.0203			

Computational Methods

The ab initio SCF–MO and MPn calculations H_3C–H···Y–I–Y⁻ (**2**, **3**) are carried out by use of the PSHONDO[15] and GAUSSIAN 86[16] programs. In our calculations the geometries of the molecular fragments CH_4 and Y–I–Y⁻ as well as the overall symmetry of H_3C–H···Y–I–Y⁻ were kept constant (i.e., C–H = 1.091 Å, ∠HCH = 109.47° in CH_4; Y–I = 2.995, 2.7705, and 2.598 Å in Y–I–Y⁻ for Y = I, Br, and Cl, respectively[17]).

(1) Williams, J. M.; Wang, H. H.; Emge, T. J.; Geiser, U.; Beno, M. A.; Leung, P. C. W.; Carlson, K. D.; Thorn, R. J.; Schultz, A. J.; Whangbo, M.-H. *Prog. Inorg. Chem.* **1987**, *35*, 51.

(2) (a) Yagubskii, E. B.; Shchegolev, I. F.; Laukhin, V. N.; Kononovich, P. A.; Kartsovnik, A. V.; Zvarykina, A. V.; Buravov, L. I. *JEPT Lett.* **1984**, *39*, 12. (b) Shibaeva, R. P.; Kaminskii, V. F.; Yagubskii, E. B. *Mol. Cryst. Liq.* Cryst. **1985**, *119*, 361. (c) Williams, J. M.; Emge, T. J.; Wang, H. H.; Beno, M. A.; Copps, P. T.; Hall, L. N.; Carlson, K. D.; Crabtree, G. M. *Inorg. Chem.* **1984**, *23*, 2558.

(3) (a) Wang, H. H.; Beno, M. A.; Geiser, U.; Firestone, M. A.; Webb, K. S.; Nunez, L.; Crabree, G. W.; Carlson, K. D.; Williams, J. M.; Azevedo, L. J.; Kwak, J. F.; Schirber, J. E. *Inorg. Chem.* **1985**, *24*, 2465. (b) Carlson, K. D.; Crabtree, G. W.; Nunez, L.; Wang, H. H.; Beno, M. A.; Geiser, U.; Firestone, M. A. Webb, K. S.; Williams, J. M. *Solid State Commun.* **1986**, *57*, 89.

(4) (a) Williams, J. M.; Wang, H. H.; Beno, M. A.; Emge, T. J.; Sowa, L. M.; Copps, P. T.; Behroozi, F.; Hall, L. N.; Carlson, K. D.; Crabtree, G. W. *Inorg. Chem.* **1984**, *23*, 3839. (b) Carlson, K. D.; Crabtree, G. W.; Hall, L. N.; Behroozi, F.; Copps, P. T.; Sowa, L. M.; Nunez, L.; Firestone, M. A.; Wang, H. H.; Beno, M. A.; Emge, T. J.; Williams, J. M. *Mol. Cryst. Liq. Cryst.* **1985**, *125*, 159.

(5) (a) Urayama, H.; Yamochi, H.; Saito, G.; Nozawa, K.; Sugano, T.; Kinoshita, M.; Sato, S.; Oshima, K.; Kawamoto, A.; Tanaka, J. *Chem. Lett.* **1988**, 55. (b) Urayama, H.; Yamochi, H.; Saito, G.; Sato, S.; Kawamoto, A.; Tanaka, A.; Mori, T.; Maruyama, Y.; Inokuchi, H. *Chem. Lett.* **1988**, 463. (c) Gärtner, S.; Gogu, E.; Heinen, I.; Keller, H. J.; Klutz, T.; Schweitzer, D. *Solid State Commun.* **1988**, *65*, 1531. (d) Carlson, K. D.; Geiser, U.; Kini, A. M.; Wang, H. H.; Montgomery, L. K.; Kwok, W. K.; Beno, M. A.; Williams, J. M.; Cariss, C. S.; Crabtree, G. W.; Whangbo, M.-H.; Evain, M. *Inorg. Chem.* **1988**, *27*, 965.

(6) Kobayashi, A.; Kato, R.; Kobayashi, H.; Moriyama, S.; Nishio, H.; Kajita, K.; Sasaki, W. *Chem. Lett.* **1987**, 495.

(7) (a) Bender, K.; Dietz, K.; Endres, H.; Helberg, H. W.; Hennig, I.; Keller, H. J.; Schäfer, H. W.; Schweitzer, D. *Mol. Cryst. Liq. Cryst.* **1984**, *107*, 45. (b) Emge, T. J.; Leung, P. C. W.; Beno, M. A.; Wang, H. H.; Williams, J. M.; Whangbo, M.-H.; Evain, M. *Mol. Cryst. Liq. Cryst.* **1986**, *138*, 393.

(8) Emge, T. J.; Wang, H. H.; Leung, P. C. W.; Rust, P. R.; Cook, J. D.; Jackson, P. L.; Carlson, K. D.; Williams, J. M.; Whangbo, M.-H.; Venturini, E. L.; Schirber, J. E.; Azevedo, L. J.; Ferraro, J. R. *J. Am. Chem. Soc.* **1986**, *108*, 695.

(9) (a) Whangbo, M.-H.; Williams, J. M.; Schultz, A. J.; Emge, T. J.; Beno, M. A. *J. Am. Chem. Soc.* **1987**, *109*, 90. (b) Whangbo, M.-H.; Williams, J. M.; Schultz, A. J.; Beno, M. A. In *Organic and Inorganic Low-Dimensional Crystalline Materials*; Delhaes, P., Drillon, M., Eds.; Plenum: New York, 1987; p 333.

(10) (a) Whangbo, M.-H.; Jung, D.; Ren, J.; Evain, M.; Novoa, J. J.; Mota, F.; Alvarez, S.; Williams, J. M.; Beno, M. A.; Kini, A. M.; Wang, H. H.; Ferraro, J. R. *The Physics and Chemistry of Organic Superconductors*; Saito, G., Kagoshima, S., Eds.; Springer-Verlag: Berlin, 1990; p 262. (b) Novoa, J. J.; Whangbo, M.-H.; Williams, J. M. *Mol. Cryst. Liq. Cryst.* **1990**, *181*, 25. (c) Whangbo, M.-H.; Novoa, J. J.; Jung, D.; Williams, J. M.; Kini, A. M.; Wang, H. H.; Geiser, U.; Beno, M. A.; Carlson, K. D. In *Organic Superconductivity*; Kresin, V. Z., Little, W. A., Eds.; Plenum: New York, 1990; p 243.

(11) (a) Laukhin, V. N.; Kostyuchenko, E. E.; Sushko, Yu. V.; Shchegolev, I. F.; Yagubskii, E. B. *JETP Lett.* **1985**, *41*, 81. (b) Murata, K.; Tokumoto, M.; Anzai, H.; Bando, H.; Saito, G.; Kajimura, K.; Ishiguro, T. *J. Phys. Soc. Jpn.* **1985**, *54*, 1236. (c) Schirber, J. E.; Azevedo, L. J.; Kwak, J. F.; Venturini, E. L.; Leung, P. C. W.; Beno, M. A.; Wang, H. H.; Williams, J. M. *Phys. Rev. B.* **1986**, *33*, 1987. (d) Schirber, J. E.; Azevedo, L. J.; Kwak, J. F.; Venturini, E. L.; Leung, P. C. W.; Beno, M. A.; Wang, H. H.; Williams, J. M. *Solid State Commun.* **1986**, *59*, 525.

(12) Wang, H. H.; Ferraro, J. R.; Carlson, K. D.; Montgomery, L. K.; Geiser, U.; Whitworth, J. R.; Schlueter, J. A.; Williams, J. M.; Hill, S.; Whangbo, M.-H.; Evain, M.; Novoa, J. J. *Inorg. Chem.* **1989**, *28*, 2267.

(13) Montgomery, L. K.; Wang, H. H.; Schleuter, J. A.; Geiser, U.; Carlson, K. D.; Williams, J. M.; Rubinstein, R. L.; Brennan, T. D.; Stupka, D. L.; Whitworth, J. R.; Jung, D.; Whangbo, M.-H. *Mol. Cryst. Liq. Cryst.* **1990**, *181*, 197.

(14) Moller, C.; Plesset, M. S. *Phys. Rev.* **1934**, *46*, 618.

(15) PSHONDO is a program written by J. P. Daudey, M. Pellissier, and J. P. Malrieu at Université Paul Sabatier, France, based upon the HONDO-76 program written by M. Dupuis, J. Rys, and H. F. King (QCPE program No. 328).

(16) Frish, M. J.; Binkley, J. S.; Schlegel, H. B.; Ragahavachari, K.; Melius, C. F.; Martin, R. L.; Stewart, J. J. P.; Bobrowicz, F. W.; Rohlfing, C. M.; Kahn, L. R.; Defrees, D. J.; Seeger, R.; Whiteside, R. A.; Fox, D. J.; Fleuder, E. M.; Pople, J. A. *Gaussian 86*; Carnegie-Mellon Quantum Chemistry Publishing Unit: Pittsburgh, PA, 1984.

(17) Novoa, J. J.; Mota, F.; Alvarez, S. *J. Phys. Chem.* **1988**, *92*, 6561.

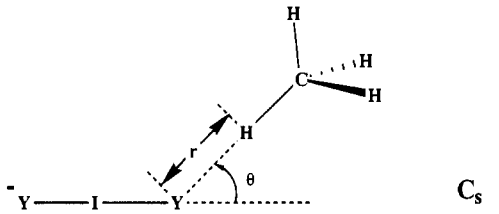

C_s

2

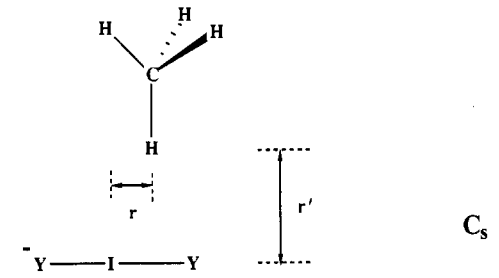

C_s

3

Potential Energy Surfaces

The potential energy surfaces of $H_3C-H\cdots Y-I-Y^-$ were obtained by performing SCF–MO calculations as a function of r and θ with model **2** and as a function of r and r' with model **3**. The calculations were carried out by use of the PSHONDO program and the basis sets described below: The carbon and hydrogen atoms were represented by the (9, 5)→[4, 2] double-ζ basis set of Dunning[18] and the (5)→[2] double-ζ set of van Duijnevelt,[19] respectively. In addition, d- and p-polarization functions were added to carbon and hydrogen, respectively (see Table I). For halogen atoms Y = I, Br, and Cl, the core electrons were described by the effective core potentials of Barthelat and Durand.[20] The valence electrons of the halogen atoms were represented by the (4, 4)→[2, 2] double-ζ set,[20] and a set of d-polarization functions were added. To properly describe the anionic nature of $H_3C-H\cdots Y-I-Y^-$, a set of s- and p-diffuse functions (with identical exponents) were also added to all the atoms other than hydrogen (Table I). This provides a well-balanced basis set of quality similar to the 3-21+G** set.

The potential energy surfaces calculated for $H_3C-H\cdots Y-I-Y^-$ are shown as energy contour diagrams in Figures 2–4 for Y = I, Br, and Cl, respectively. These contour diagrams were generated by fitting the SCF–MO energies with cubic spline functions. These figures show that the $H_3C-H\cdots Y-I-Y^-$ systems are all bound, and the C–H bond prefers to make a short contact with the terminal halogen atoms of $Y-I-Y^-$. The optimum H···Y distances (r_{opt}), the optimum contact angles (θ_{opt}), and the binding energies ΔE calculated for these systems are summarized in Table II. Figures 2–4 reveal that the potential energy surfaces are soft with respect to the variation of the contact angle θ (0–90°), and the energetic tendency for a C–H bond to make a short contact with the terminal halogen of $Y-I-Y^-$ increases as Y varies from I to Br to Cl, in agreement with the expected hydrogen-bonding abilities of the halogen atoms. The latter finding is reasonable, since a C–H bond has a partial positive charge on hydrogen and since the distribution of the partial negative charge, largely localized at the terminal halogen atoms, becomes more contracted as Y changes from I to Br to Cl. This finding is also consistent with the observation from Figure 1 that the number of the short C–H···anion contacts involving the middle halogen atom of $Y-I-Y^-$ decreases as Y varies from I to Br to Cl. Although the potential energy surfaces of Figures 2–4 are soft, it is noted that the interaction of a C–H bond with the I_3^- and IBr_2^- anions prefers a nonlinear approach ($\theta_{opt} > 0°$), while that with the anion ICl_2^- prefers a linear arrangement ($\theta_{opt} = 0°$).

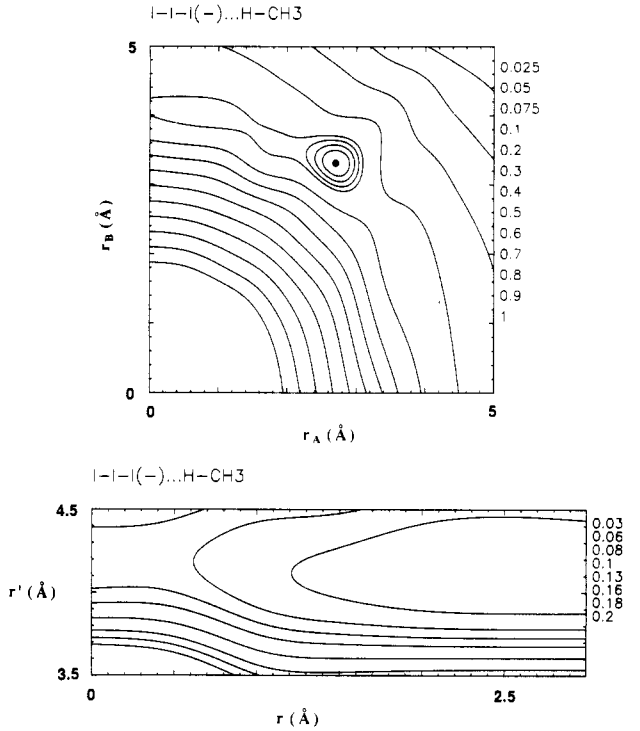

Figure 2. Calculated potential energy surface for $H_3C-H\cdots I-I-I^-$ using (a, top) model **2**, where $r_A = r\cos\theta$ and $r_B = r\sin\theta$ and (b, bottom) model **3**. The minimum energy point is represented by a filled circle, and the values of the energy contours plotted (in kcal/mol with respect to the minimum energy point) are shown in the right-hand-side margins of the diagrams.

Table II. Optimum H···Y Distance, r_{opt}, Optimum H···Y Contact Angle, θ_{opt}, and Binding Energy, ΔE, Calculated for $H_3C-H\cdots Y-I-Y^-$ at the SCF–MO Level

anion X^-	r_{opt}, Å	θ_{opt}, deg	ΔE, kcal/mol
$I-I-I^-$	4.087	79.0	0.41
$Br-I-Br^-$	3.719	69.2	0.48
$Cl-I-Cl^-$	3.434	0.0	0.57

Table III. Optimum H···Y Distance, r_{opt}, Binding Energy, ΔE, Zero-Point Corrected Binding Energy, ΔE_0, and Stretching Frequency, ν_{st}, Calculated for $H_3C-H\cdots I-I-I^-$ at the SCF–MO and the MP*n* Levels by Using the 3-21+G** Quality Basis Sets

	SCF	MP2	MP3	MP4
r_{opt}, Å	4.060	3.500	3.550	3.513
ΔE, kcal/mol	0.35	1.13	1.05	1.14
ΔE_0, kcal/mol	0.32	1.07	0.99	1.08
ν_{st}, cm^{-1}	23.60	41.2	42.9	41.8

C–H···Anion Interaction Energies

The results presented in the previous section do not include correlation energy, which is expected to be important in describing weak intermolecular interactions. To more accurately estimate the interaction energies associated with $H_3C-H\cdots Y-I-Y^-$, we perform ab initio calculations at the MP*n* (n = 2–4) level. Since the potential energy surfaces of the $H_3C-H\cdots Y-I-Y^-$ systems are soft with respect to the θ change (0–90°), we adopt the θ_{opt} values obtained in the previous section and only optimize the H···Y contact distances. These SCF–MO/MP*n* calculations are performed by using the GAUSSIAN 86 program with the 3-21+G** basis set for CH_4 and with a similar quality basis set for the valence orbitals of I, Br, and Cl (i.e., the [2, 2] contracted set obtained from (3, 3) supplemented with the same polarization and diffuse functions listed in Table I) and the effective core potentials of Wadt and Hay[21] for the core electrons of I, Br, and Cl. For

(18) Dunning, T. M. *J. Chem. Phys.* **1970**, *53*, 2823.
(19) van Duijneveldt, F. B. IBM Technical Research Report No. RJ 945; IBM: Armonk, NY, 1971.
(20) Barthelat, J. C.; Durand, Ph. *Gazz. Chim. Ital.* **1978**, *108*, 225.

Table IV. Optimum H···Y Distance, r_{opt} (Å), Binding Energy, ΔE (kcal/mol), Basis Set Superposition Error Corrected Binding Energy, ΔE_{cp} (kcal/mol), and the Stretching Vibrational Frequency, ν_{st} (cm^{-1}), Calculated for $H_3C-H\cdots Y-I-Y^-$ at the SCF-MO and the MP2 Levels by Using the 3-21+G** and 3-21++G** Basis Sets

		SCF-MO				MP2			
basis set	anion	r_{opt}	ΔE	ΔE_{cp}	ν_{st}	r_{opt}	ΔE	ΔE_{cp}	ν_{st}
3-21+G**	I-I-I^-	4.060	0.35	0.27	23.60	3.500	1.13	0.70	41.17
	Br-I-Br^-	3.634	0.48	0.36	23.45	3.144	1.27	0.72	44.41
	Cl-I-Cl^-	3.293	0.66	0.45	39.74	2.848	1.58	0.79	75.87
3-21++G**	I-I-I^-	4.031	0.36	0.27	22.45	3.358	1.48	0.60	47.88
	Br-I-Br^-	3.510	0.59	0.24	27.66	3.102	1.81	0.73	70.50
	Cl-I-Cl^-	3.300	0.81	0.43	37.43	2.821	2.18	0.77	75.74

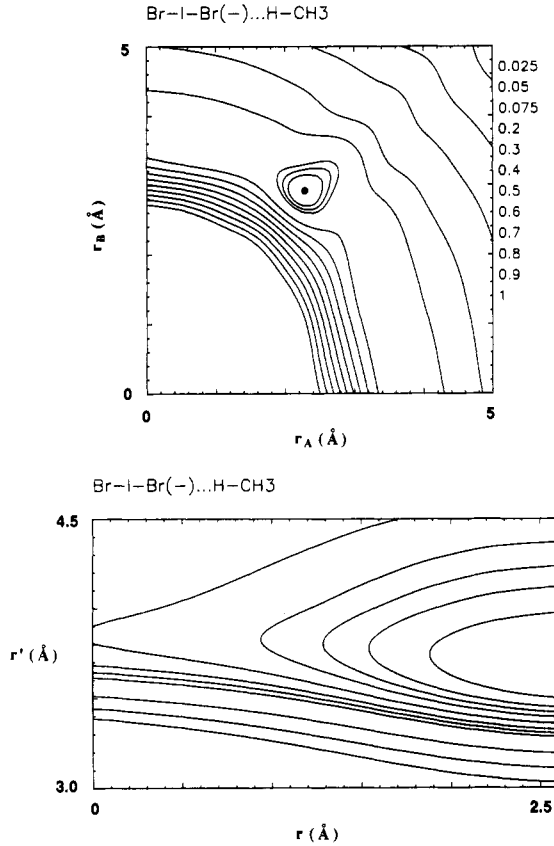

Figure 3. Calculated potential energy surface for $H_3C-H\cdots Br-I-Br^-$ using (a, top) model **2**, where $r_A = r\cos\theta$ and $r_B = r\sin\theta$ and (b, bottom) model **3**. The minimum energy point is represented by a filled circle, and the values of the energy contours plotted (in kcal/mol with respect to the minimum energy point) are shown in the right-hand-side margins of the diagrams.

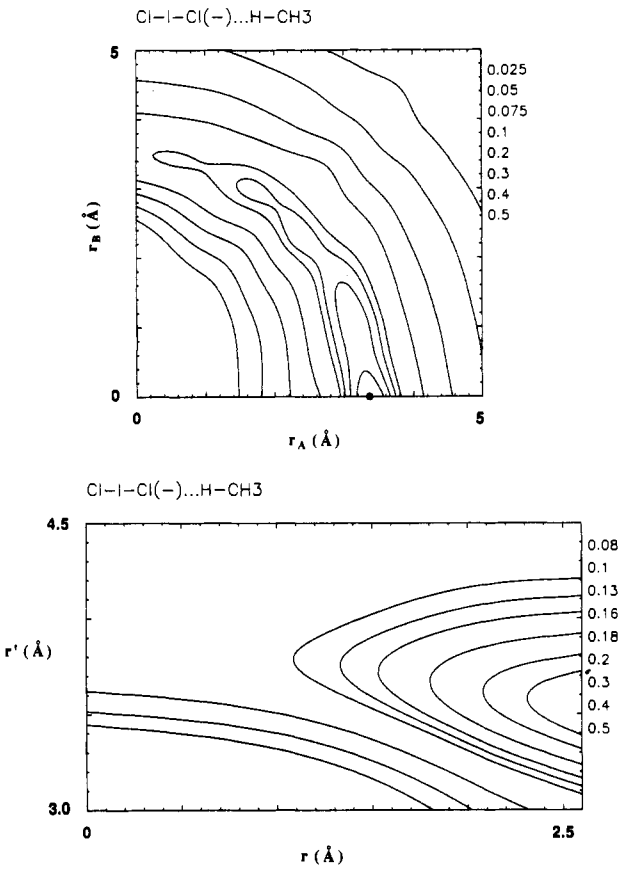

Figure 4. Calculated potential energy surface for $H_3C-H\cdots Cl-I-Cl^-$ using (a, top) model **2**, where $r_A = r\cos\theta$ and $r_B = r\sin\theta$ and (b, bottom) model **3**. The minimum energy point is represented by a filled circle, and the values of the energy contours plotted (in kcal/mol with respect to the minimum energy point) are shown in the right-hand-side margins of the diagrams.

convenience, this basis set for the halogen atoms will be referred to as the 3-21+G** set. In our study one additional basis set, i.e., 3-21++G**, is also employed. This set is obtained by adding an s-diffuse function (with exponent of 0.036) on H to the 3-21+G** set.

Correlation Level

The first two rows of Table III list the r_{opt} and ΔE values calculated for $H_3C-H\cdots I_3^-$ at the SCF-MO level. These values are close to the corresponding ones of Table II, so that the basis sets and the pseudopotentials used in our GAUSSIAN 86 calculations provide results comparable to those obtained from our PSHONDO calculations. The r_{opt} and ΔE values of $H_3C-H\cdots I_3^-$ calculated by the MP*n* (n = 2–4) method are also listed in Table III. This table reveals that correlation energy shortens the r_{opt} values and increases the binding energies ΔE. It is noted that the MP2 and MP4 methods give similar r_{opt} and ΔE values. The harmonic stretching frequencies (ν_{st}) of $H_3C-H\cdots I_3^-$ (Table III), calculated under the assumption that CH_4 and I_3^- behave as a pseudoparticle on the calculated potential energy curve, also suggest that the MP2 and MP4 potential surfaces around r_{opt} are quite similar. Consequently, the MP2 method seems adequate for investigating the nature of the C-H···Y-I-Y^- (Y = I, Br, Cl) interactions in $H_3C-H\cdots Y-I-Y^-$. Also shown in Table III is the binding energy corrected with the zero-point vibrational frequency ν_{st} at each MP*n* (n = 2–4) level (i.e., $\Delta E_0 = \Delta E - \nu_{st}/2$, when ν_{st} is expressed in kcal/mol). These ΔE_0 values are very close to the corresponding ΔE values.

The potential energy curves calculated for $H_3C-H\cdots I-I-I^-$ (θ_{opt} = 79.0°) at the SCF-MO and the MP2 levels are essentially similar in shape, except that correlation energy makes r_{opt} smaller and ΔE larger. Since the $H_3C-H\cdots Y-I-Y^-$ system has a large HOMO–LUMO gap, the single reference method of correlation energy calculation such as the MP*n* would be adequate for studying the interaction energies of these systems. Further, the qualitative features of their potential energy surfaces discussed in the previous section are not expected to change by correlation energy calculations.

Interaction Energies

Table IV summarizes the r_{opt}, ΔE, and ν_{st} values calculated for $H_3C-H\cdots Y-I-Y^-$ (Y = I, Br, Cl) at the SCF-MO and MP2 levels

(21) Wadt, W. R.; Hay, P. J. *J. Chem. Phys.* **1985**, *82*, 284.

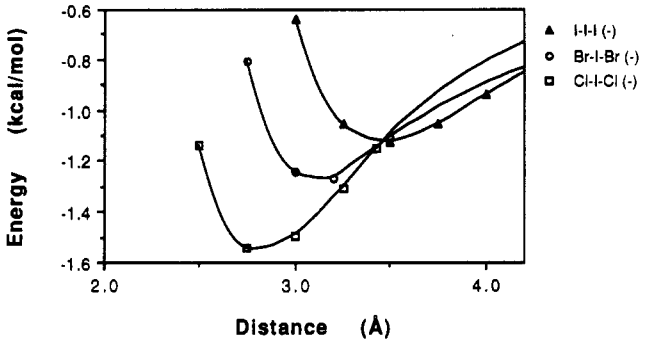

Figure 5. Potential energy curves calculated for $H_3C-H\cdots Y-I-Y^-$ at the MP2 level by using the 3-21+G** quality basis set.

by using the 3-21+G** and 3-21++G** basis sets. For all the $H_3C-H\cdots Y-I-Y^-$ systems, correlation energy shortens r_{opt} and increases ΔE with all the basis sets. In addition, the ΔE value for each system is slightly larger with the 3-21++G** set. The binding energy ΔE between CH_4 and $Y-I-Y^-$ increases as Y varies from I to Br to Cl. The r_{opt} values of the H···Y contacts calculated for $H_3C-H\cdots Y-I-Y^-$ are close to their expected van der Waals (VDW) contact distances (i.e., H···Y = 3.15, 3.00, and 2.90 Å for Y = I, Br, and Cl, respectively). The MP2 results of Table IV show that the deviation of r_{opt} from the VDW contact distance decreases on going from H···I to H···Br to H···Cl. The r_{opt} value is larger than the VDW contact distance for H···I and H···Br but smaller for H···Cl. In addition, the calculated interaction energies for the H···Y contacts increase in magnitude as Y varies from I to Br to Cl. All these findings can be explained in terms of the expected hydrogen-bonding ability of the halogen atom Y, which should increase as Y changes from I to Br to Cl. In the organic donor salts with trihalide anions there occur numerous hydrogen···halogen contacts whose contact distances lie in the vicinity of their VDW contact distances.[1] Some of those contacts are shorter than the VDW distances by about 0.3–0.4 Å. [For examples, H···I = 2.966 Å in β-(BEDT-TTF)$_2$AuI$_2$ at 20 K,[1,9a] H···Br = 2.887 Å in β-(BEDT-TTF)$_2$IBr$_2$ at 9 K,[9a] and H···Cl = 2.59 Å in β-(BEDT-TTF)$_2$ICl$_2$ at 120 K.[1]] This is due most likely to the effect of Coulombic attraction between anion layers and partially oxidized donor molecule layers.

We have estimated the basis set superposition errors (BSSE) on the basis of the counterpoise method. The binding energies corrected by this method, i.e., ΔE_{cp}, are also listed in Table IV. These ΔE_{cp} values show that the $H_3C-H\cdots Y-I-Y^-$ systems are bound with all the basis set. Whether or not the ΔE_{cp} values are more meaningful than the ΔE values has been a subject of controversy.[22] In our discussion, therefore, we will focus on our ΔE values.

Figure 5 shows the potential energy curves calculated for the $H_3C-H\cdots Y-I-Y^-$ systems with the 3-21+G** basis set. The ν_{st} values of Table IV and Figure 5 show that the potential well for the $C-H\cdots Y-I-Y^-$ interaction becomes deeper and stiffer as Y changes form I to Br to Cl. This reflects the fact that the charge distribution around Y in the anion $Y-I-Y^-$ becomes more contracted as Y varies from I to Br to Cl. The binding energies of $H_3C-H\cdots Y-I-Y^-$ (Y = I, Br, Cl) associated with their C–H···Y contacts are estimated to be of the order of 1–2 kcal/mol. Obviously, these energies are considerably smaller than the typical hydrogen-bonding energy (~6 kcal/mol)[23] associated with an O–H···O contact. However, they are considerably greater than the binding energy associated with a C–H···H–C contact, which is estimated to be about 0.1–0.2 kcal/mol according to the MP2 level calculations of $H_3C-H\cdots H-CH_3$.[24] In the absence of strong intermolecular contact interactions such as O–H···O found in regular hydrogen-bonded systems and in the presence of very weak intermolecular contact interactions[10] such as S···S and Se···Se, the C–H···anion interaction energies of 1–2 kcal/mol are crucial in determining the crystal packing patterns of organic charge-transfer salts and hence their electronic properties as well.

Concluding Remarks

Our ab initio MP2 level calculations on the model systems $H_3C-H\cdots Y-I-Y^-$ (Y = I, Br, Cl) show that the $H_3C-H\cdots Y-I-Y^-$ systems are all bound, and their binding energies are not strongly affected by the change in the C–H···Y contact angle θ. The C–H bond prefers to make a short contact with the terminal halogen atoms of $Y-I-Y^-$, and this tendency increases as Y varies from I to Br to Cl in agreement with the expected hydrogen-bonding abilities of the halogen atoms. The potential energy curve of the $C-H\cdots Y-I-Y^-$ interaction becomes deeper and stiffer as Y changes from I to Br to Cl. The binding energies of the $C-H\cdots Y-I-Y^-$ interactions are estimated to be of the order of 1–2 kcal/mol. The C–H···anion interaction energies of this order of magnitude are expected to be crucial in governing the crystal packing patterns of organic charge-transfer salts.

Acknowledgment. Work at North Carolina State University and Argonne National Laboratory is supported by the U.S. Department of Energy, Office of Basic Energy Sciences, Division of Materials Science, under Grant DE-FG05-86ER45259 and Contract W-31-109-ENG-38, respectively. We express our appreciation for computing time on the ER-Cray computer made available by the DOE, on the VAX-8700 computer at Argonne National Laboratory provided by the Chemistry Division, and on the VAX 6320 computer made available by DGICYT Grant PB89-0268 (Spain). J.J.N. thanks NATO and the Ministerio de Educacion y Ciencia (Spain) for Fellowships that made it possible to visit North Carolina State University.

(22) (a) Schwenke, D.; Truhlar, D. G. *J. Chem. Phys.* **1985**, *82*, 2418; **1986**, *84*, 4113. (b) Colins, J. R.; Gallup, G. A. *Chem. Phys. Lett.* **1986**, *123*, 56. (c) Loushin, S. K.; Liu, S.-Y.; Dykstra, C. E. *J. Chem. Phys.* **1986**, *84*, 2720. (d) Cybulski, S. M.; Chalasinski, G.; Moszynski, R. J. *Chem. Phys.* **1990**, *92*, 4357.

(23) Hobza, P.; Zahradnik, R. *Top. Curr. Chem.* **1980**, *93*, 53.

(24) Novoa, J. J.; Whangbo, M.-H., Williams, J. M. Manuscript in preparation.